Langmuir

LETTER

pubs.acs.org/Langmuir

Hybrid Macroscopic Fibers from the Synergistic Assembly Between Silica and Filamentous Viruses

Eric Grelet,* Alexandra Moreno, and Rénal Backov

Centre de Recherche Paul-Pascal, CNRS - Université de Bordeaux, 115 Avenue Albert Schweitzer, 33600 Pessac, France

ABSTRACT: In this work, we report the elaboration of macroscopic hybrid virus−silica fibers. By using a silicate sol as inorganic precursor combined with the filamentous *fd* virus, well-dispersed hybrid fibers are obtained in solution. These macroscopic *fd*−silica fibers exhibit a narrow distribution of their diameter, while their length is at the millimeter scale. A scenario of the morphosynthesis is proposed to account for the formation of these high aspect ratio hybrid fibers.

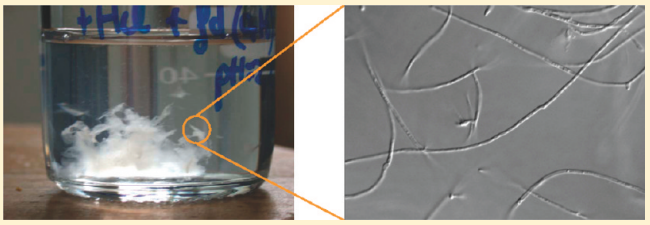

INTRODUCTION

An abundance of composite biominerals exists in nature whose complexity gives rise to enhanced material properties. Oysters, corals, and diatoms are examples of living organisms who construct complex biominerals essential to their survival.[1−5] The control and function of biominerals evolved by these organisms naturally leads to the desire to engineer such architectures by understanding and harnessing the power of biomineralization. A fundamental aspect is the study of biological mineralization that combines supramolecular assemblies with mineralization in order to address the key parameters occurring at the organic−inorganic interfaces. This concerns for instance nucleation mechanisms, growth regimes, and polymorphism of inorganic matter. In such context, biological templates, such as viruses, ferritin, and self-assembled protein complexes, allow genetic programmability and site-specific chemistry, providing thereby a land of opportunities for the fabrication of novel materials with original functionalities. Genetically engineered and chemically modified viruses have been used extensively to direct material synthesis by controlling composition, mutation positions, and morphologies.[6−11] This work focuses on the elaboration of long, thin macroscopic hybrid fibers with large length to width aspect ratio by using one-dimensional (1D) self-organization of the filamentous *fd* virus. Such unidimensional microstructures exhibiting anisotropic properties have a high interest in different research areas, such as for instance electronics or optics.[12]

RESULTS AND DISCUSSION

The *fd* bacteriovirus is a charged monodisperse rodlike particle with a high aspect ratio (contour length of 880 nm and diameter of 6.6 nm). This biological polyelectrolyte is semiflexible (persistence length of 2.8 μm) and has a molecular weight of $M_W = 1.64 \times 10^7$ g/mol.[13] *Fd* is formed by a single stranded DNA, around which about 2700 identical coat proteins are helicoidally wrapped following a 5-fold rotation axis combined with a 2-fold screw axis.[14,15] A representation of the *fd* virus surface is given in Scheme 1. Due to the rodlike shape of the bacteriovirus, aqueous *fd* suspensions have been shown to depict different self-organized states: isotropic liquid, chiral nematic,[16] smectic,[17] columnar, and crystalline phases,[18] by increasing the *fd* virus concentration.

Scheme 1. Electron Microscopy Image of the *fd* Virus (top) Which Exhibits a Length of 880 nm and a Diameter of 6.6 nm and Schematic All-Atom Representation of Its Surface (bottom)[14,16] *a*

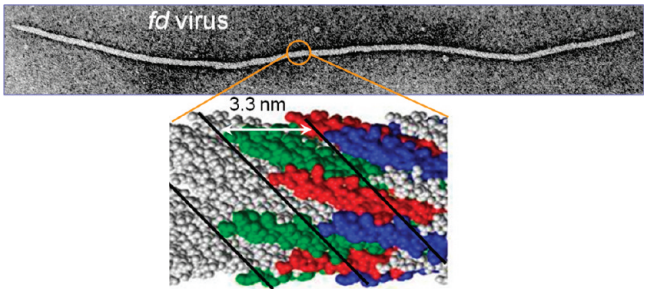

a Proteins with a given color are related by a 5-fold symmetry axis. The distance of 3.3 nm corresponds to the protein periodicity along the capsid.

Each coat protein is formed by 50 amino acids, which results in a net charge (carried by ionic amino acids) of about −3e per protein in water at neutral pH, corresponding to a linear charge density of about 10e/nm on the virus.[19] The *fd* virus isoelectric point is at pH = 4.2, above which the virus surface is negative while being positive below.[19] This has to be compared with the silica isoelectric point being at pH 2.1.[20] Therefore, a small pH window exists, between pH = 2.1 and pH = 4.2, where positive silica clusters attract negatively charged viruses electrostatically.

Received: February 25, 2011
Revised: March 23, 2011
Published: March 29, 2011

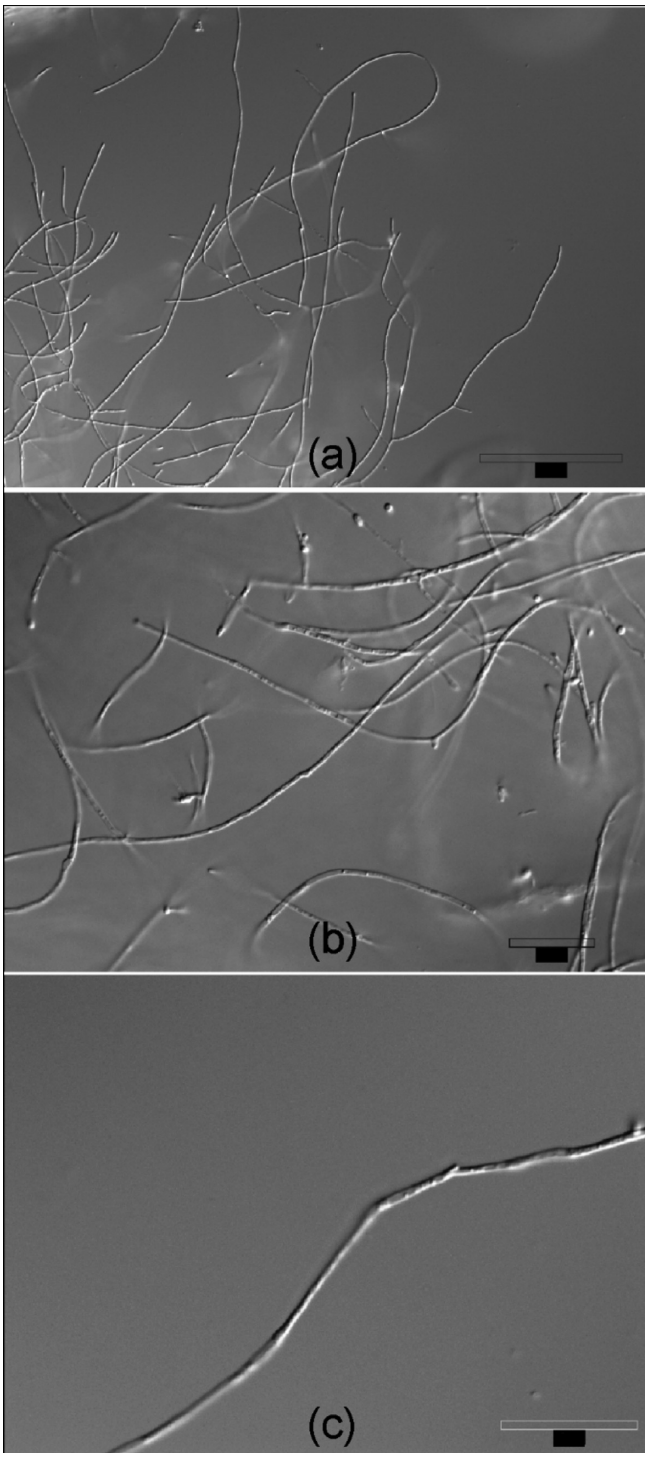

Figure 1. As-synthesized hybrid *fd*−silica fibers observed in solution by optical differential interference contrast microscopy at different magnifications. Note the outstanding homogeneity and uniformity in diameter of these macroscopic fibers. The white scale bars indicate 100 μm in (a) and 20 μm in (b) and (c).

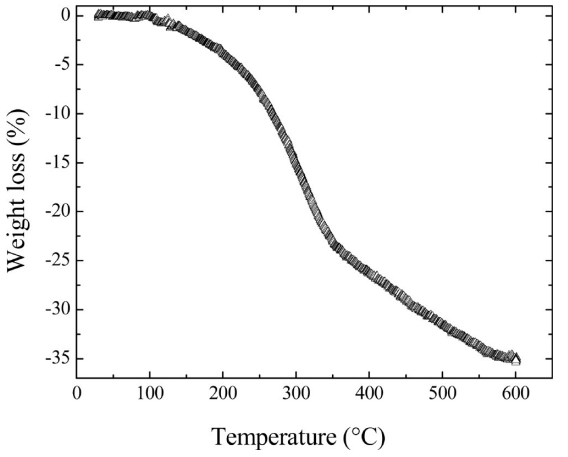

Figure 2. Thermal gravimetric analysis experiment performed on the washed hybrid fibers. The heating rate was 2 °C/min.

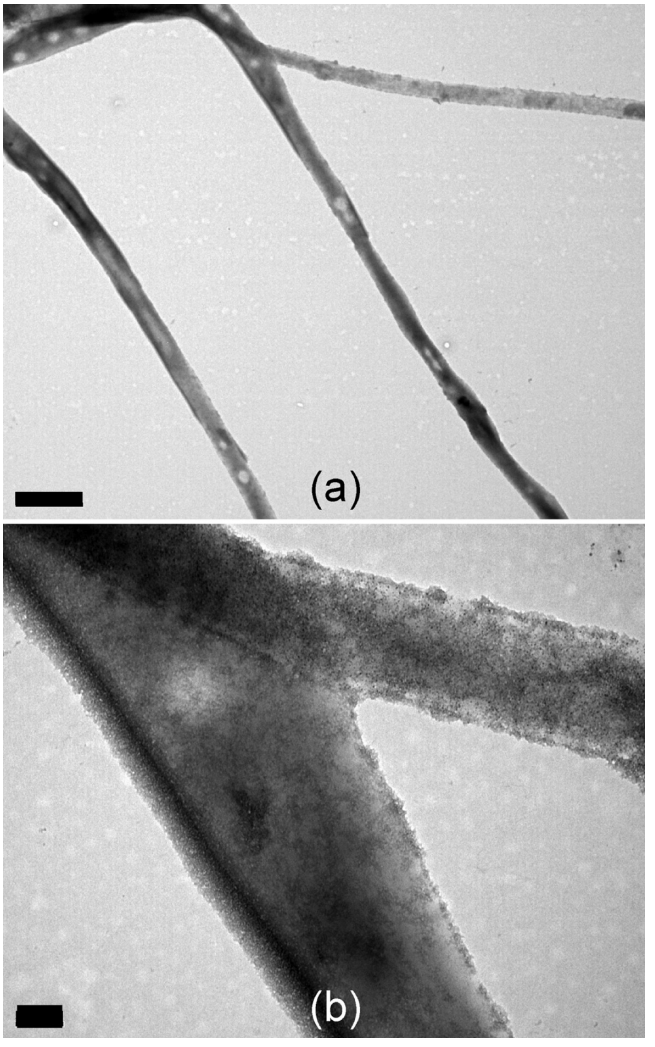

Figure 3. TEM images of the hybrid *fd*−silica fibers. The scale bar represents 2 μm in (a) and 200 nm in (b).

Our target for synthesis was aimed at pH = 3 to take advantage of these attractive interactions (see Experimental Section for details). The usual approach to silica mineralization involving tetraethoxyorthosilane (TEOS)[21−24] can induce virus damage due to ethanol release during the TEOS hydrolysis. As an alternative, we have developed a synthetic pathway based on a silicate solution as the inorganic source. With this synthetic

dx.doi.org/10.1021/la200743n |*Langmuir* 2011, 27, 4334–4338

Scheme 2. Overall Hypothesized Scenario That Depicts Hybrid *fd*—Silica Fiber Generation[a]

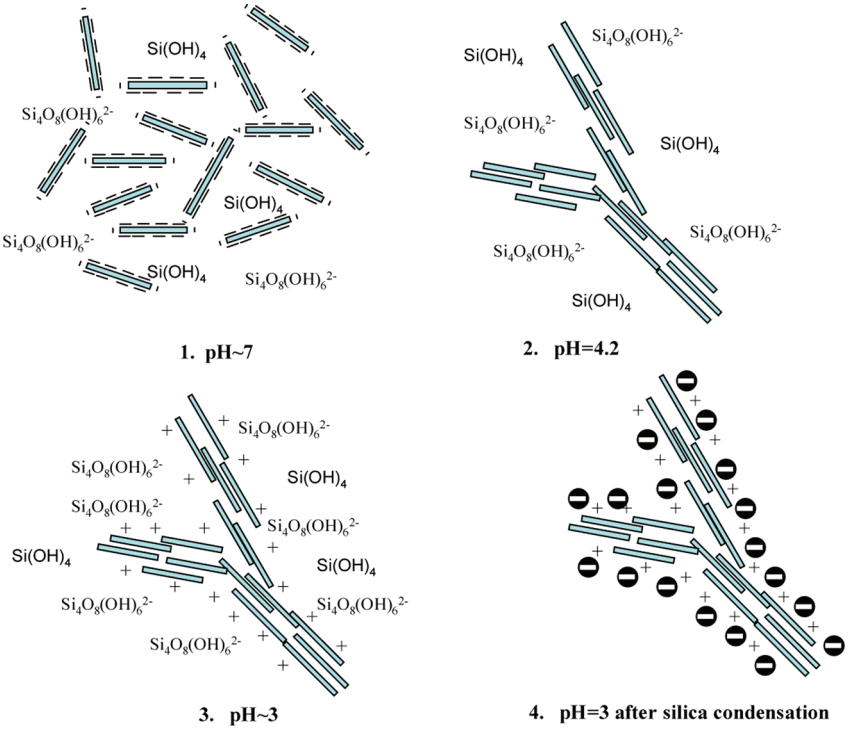

[a] For clarity issue, the positive sodium counterions observed have been neglected within the scheme. The solid circle bar symbols represent the negatively charged silica nanoparticles.

process, we succeeded in generating well-dispersed macroscopic fibers up to a few millimeters in length that can easily be seen at the optical scale (Figure 1).

This observed mineralization suggests a synergistic assembly of the negatively charged silica particles and the positively charged *fd* virus. The hybrid *fd*—silica fibers were rinsed with ethanol at the end of the synthesis to remove any chemical and biological residues. In order to confirm the hybrid organic—inorganic character of the fibers, thermal gravimetric analysis (TGA) was performed in air. TGA experiments revealed a total organic and water loss of 35 wt % associated with this hybrid compound (Figure 2), where the water weight loss up to 200 °C is found to be 3.6 wt %. Despite the severe alcohol washing, we can see that these hybrid fibers are composed of about 31 wt % of organic matter, leading to the following stoichiometry $(\text{virus})_1(SiO_2)_x \cdot (0.19H_2O)_x$ with $x = 5.7 \times 10^5$. The fact that the organic content survived the ethanol washing process means that the silica matrix is protecting the organic content, indicating that most of the organic matter is embedded within the silica matrix. This was confirmed by subsequent transmission electron microscopy (TEM) experiments shown in Figure 3b, which indicate a diffuse fractal interface of the fibers, as a result of the typical silica condensation performed in acid conditions.[20]

One of the outstanding features of the hybrid *fd*—silica fibers reported in this work is their uniformity in diameter observed along single fibers, and the narrow diameter distribution (from 0.5 to 2 μm) between different fibers as shown in both optical (Figure 1) and electron (Figure 3) microscopy experiments. This feature obtained for macroscopic fibers differs from other works, where usually some polydispersity was observed as a consequence of the bundling of nanofibers into macroscopic dense aggregates.[21,22] The diameter range of the hybrid fibers indicates that the imbedded viruses lie parallel to the long axis of the fiber since the diameter could not accommodate the virus length.

Reaching a pH of 4.2 (corresponding to the *fd* virus isoelectric point) promotes rapid virus aggregation through attractive van der Waals interactions. Note that viruses alone in solution at the isoelectric point only form statistical aggregates without any specific shape. This demonstrates the *synergistic* assembly between viruses and silica to obtain such macroscopic hybrid fibers. If the pH is further decreased below 4.2, the virus become positively charged, and compensated by the growing silica clusters negatively charged.[20]

A second important feature of the hybrid *fd*—silica fibers is the observation that they are well-dispersed in solution with only a few branching points rather than being aggregated in bundles after synthesis (Figure 1). When using TEOS as precursor within this range of pH, the polycondensation generates a polymeric network bearing a strong fractal character.[20] Therefore hybrid fibers we have synthesized with TEOS are connected and stacked on each other. Conversely, when using charged silicate as the inorganic precursor, the kinetics of electrostatically induced aggregation between the *fd* virus and silicate is certainly faster than the polycondensation itself, thereby inducing enhanced heterogeneous nucleation at the organic—inorganic interface. Thus, working with silicate as the inorganic source instead of TEOS circumvents macroscopic fiber aggregation. The TEM experiments (Figure 3b) unambiguously show that the silica network is present at the outer part of the fibers, thereby repulsing other negatively charged silica coated fibers.

Silica growth occurs preferentially at the surface of the organic viruses rather than in the bulk solution, because the virus surface acts as heterogeneous nucleation sites where the nucleation enthalpy is minimized. Moreover, the positive charge at the virus

dx.doi.org/10.1021/la200743n |*Langmuir* 2011, 27, 4334–4338

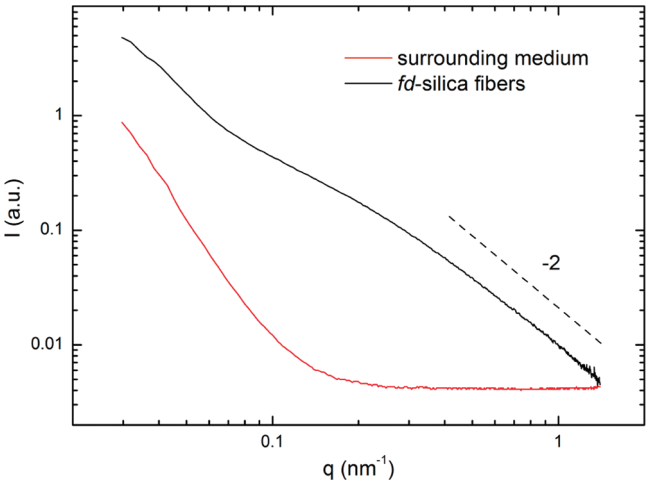

Figure 4. SAXS intensity as a function of the scattering wave vector q for the hybrid *fd*−silica fibers (black line) and the aqueous surrounding medium (red line) after washing with ethanol. For comparison, the dashed line represents a power-law decay with an exponent of −2.

surface induces a local increase of negatively charged silicate precursors. This synergistic assembly stops only when the fibers become macroscopically electroneutral. At that point, if the electroneutrality is the main factor governing the as-proposed synergistic assembly and not the intrinsic silica heterogeneous polycondensation, then the yield of silica condensation within the hybrid fibers should not necessarily be equal to 100%. At the beginning of the fiber synthesis, the molar ratio of silicate to virus is 9.3×10^5 whereas the ratio of silica to virus on the final hybrid fibers is 5.7×10^5, meaning that approximately 61% of the silicate precursors in solution condense on the viruses to form hybrid fibers. The fact that macroscopic electroneutrality of the fiber is governing the synergistic virus assembly/silica polycondensation is indeed certainly the reason why the native hybrid fibers obtained by a bottom-up approach are bearing a narrow distribution with regard to their microscopic diameters (Figure 1). Based on these considerations, a first scenario of the morphosynthesis is depicted in Scheme 2, although the detailed quantitative mechanisms have still to be elucidated.

The *fd*−silica fiber formation does not involved organic−inorganic deep interaction at the molecular levels. Considering Fourier transform infrared spectroscopy (FTIR) investigations, the SiO stretching mode occurring at 1200 cm^{-1} is masking the organic vibration modes, and this is why no specific organic−inorganic interaction has been evidenced.

Small angle X-ray scattering (SAXS) experiments have been performed on the *fd*−silica fibers (from which the contribution of the aqueous surrounding medium has been subtracted), and the scattered intensity is plotted in Figure 4. In the regime of wave vectors studied here where $q \gg 1/\Phi$ with Φ being the fiber diameter, the scattered intensity should follow Porod's law ($I \propto q^{-4}$) if a sharp interface exists between the fiber surface and the solvent. Such behavior cannot be evidenced, indicating a diffuse interface at the surface fiber, as confirmed by TEM experiment (Figure 3b). This diffuse interface most probably originates from a diffusion limited aggregation process generating a fractal structure.[23] This could explain the lower decay (compared to Porod's law) of the scattered intensity observed in Figure 4.

In conclusion, we describe the morphosynthesis of hybrid macroscopic fibers based on a synergistic assembly between *fd* virus and silica leading to an organic core embedded within a silica shell. Contrary to other synthetic pathways,[21,22,24−26] this route based on silicate precursors allows the formation of homogeneous *macroscopic* fibers[27] and not bundles of nanofibers.[21,22] An overall scenario of the morphosynthesis is hypothesized to account for the formation of these hybrid macroscopic fibers.

EXPERIMENTAL SECTION

Products. Silicate solution (27% wt) was purchased from Sigma Aldrich (pH 9.4).

Synthesis. Virus suspensions with a concentration of 0.16 mg/mL are first prepared following standard biological protocols,[28] along with a dilute silicate solution at 0.27% wt. In the second step, 122 mL of the dilute silicate solution is mixed with 13 mL of the virus solution. Finally, the pH is brought to 2.5 using 0.1 M HCl. The final solution is stirred for 1 h and then left without stirring for 3 days, after which some entangled fibers are visible by eye (see the Abstract graphic). Those fibers are extracted from the bulk using a Pasteur pipet and first washed three times with deionized water. To ensure that the fibers are not exclusively organic matter, they were then washed three more times with absolute ethanol before TGA, electronic microscopy, and SAXS investigations.

Characterization. TGA measurements were carried out in air (flux 5 cm^3/min), using a heating rate of 2 °C/min on a Stearam TAG-1750 thermogravimetric analyzer. FTIR spectra were obtained with a Nicolet 750 FTIR spectrometer. TEM was performed using a HITACHI − H7650 transmission electron microscope operating at 80 kV equipped with an ORIUS GATAN (11MPX) camera. SAXS measurements on hybrid *fd*−silica fibers placed in quartz capillary tubes were obtained at the ID02 beamline at the European Synchrotron Radiation Facility (Grenoble, France), working with a wavelength of 0.995 Å and a sample-to-detector distance of 3.01 m. Optical microscopy experiments were performed in transmission using an IX71-Olympus microscope working with differential interference contrast.

AUTHOR INFORMATION

Corresponding Author

*E-mail: grelet@crpp-bordeaux.cnrs.fr.

ACKNOWLEDGMENT

We would like to thank Alain Derré and Isabelle Ly for their help in the TGA and TEM experiments, respectively, Emilie Pouget, and Joshua Blouwolff for helpful discussions and for the critical reading of the manuscript.

REFERENCES

(1) Mann, S. *Angew. Chem., Int. Ed.* **2000**, *39*, 3393–3406.
(2) Lowenstam, H. A.; Weiner, S. *On Biomineralyzation*; Oxford University Press: New York, 1989.
(3) Mann, S.; Webb, J.; Williams, R. J. P. *Biomineralyzation Chemical and Biochemical Perspectives*; Wiley-VCH: Weinheim, 1989.
(4) Jones, F.; Cölfen, H.; Antonietti, M. *Colloid Polym. Sci.* **2000**, *278*, 491–501.
(5) Xu, A.-W.; Ma, Y.; Cölfen, H. *J. Mater. Chem.* **2007**, *17*, 415–449.
(6) Lee, S.-W.; Mao, C.; Flynn, C. E.; Belcher, A. M. *Science* **2002**, *296*, 892–895.
(7) Douglas, T.; Young, M. *Nature* **1998**, *393*, 152–155.
(8) Wang, Q.; Lin, T.; Tang, L.; Johnson, J. E.; Finn, M. G. *Angew. Chem., Int. Ed.* **2002**, *114*, 477–480.

(9) Douglas, T.; Young, M. *Science* **2006**, *312*, 873–875.
(10) Mao, C.; Solis, D. J.; Reiss, B. D.; Kottmann, S. T.; Sweeney, R. Y.; Hayhurst, A.; Georgiou, G.; Iverson, B.; Belcher, A. M. *Science* **2004**, *303*, 213–217.
(11) Nam, K. T.; Kim, D.-W.; Yoo, P. J.; Chiang, C. Y.; Meethong, N.; Hammond, P. T.; Chiang, Y.-M.; Belcher, A. M. *Science* **2006**, *312*, 885–888.
(12) Huang, Y.; Duan, X.; Wei, Q.; Lieber, C. M. *Science* **2001**, *291*, 630–633. Baughmann, R. H.; Zakhidov, A. A.; de Heer, W. A. *Science* **2002**, *297*, 787–792. Melosh, N. A.; Boukai, A.; Diana, F.; Gerardot, B.; Badolato, A.; Petroff, P. M.; Heath, J. R. *Science* **2003**, *300*, 112–115.
(13) Barry, E.; Beller, D.; Dogic, Z. *Soft Matter* **2009**, *5*, 2563–2570.
(14) Marvin, D. A.; Welsh, L. C.; Symmons, M .F.; Scott, W. R. P.; Straus, S. K. *J. Mol. Biol.* **2006**, *355*, 294–309.
(15) Bhattacharjee, S.; Glucksman, M. J.; Makowski, L. *Biophys. J.* **1992**, *61*, 725–735. Zeri, A. C.; Mesleh, M. F.; Nevzorov, A. A.; Opella, S. J. *Proc. Natl. Acad. Sci. U.S.A.* **2003**, *100*, 6458–6463.
(16) Tombolato, F.; Ferrarini, A.; Grelet, E. *Phys. Rev. Lett.* **2006**, *96*, 258302.
(17) Dogic, Z.; Fraden, S. *Phys. Rev. Lett.* **1997**, *78*, 2417–2420. Lettinga, M. P.; Grelet, E. *Phys. Rev. Lett.* **2007**, *99*, 197802.
(18) Grelet, E. *Phys. Rev. Lett.* **2008**, *100*, 168301.
(19) Zimmermann, K.; Hagedorn, H.; Heuck, C. C.; Hinrichsen, M.; Ludwig, H. *J. Biol. Chem.* **1986**, *261*, 1653–1655.
(20) Brinker, C. J.; Scherer, G. W. *Sol-Gel Science: the Physics and Chemistry of Sol-Gel Processing*; Academic Press: San Diego, 1990.
(21) Zhang, Z.; Buitenhuis, J. *Small* **2007**, *3*, 424–428.
(22) Gole, J. L.; Wang, Z. L.; Dai, Z. R.; Stout, J.; White, M. *Colloid Polym. Sci.* **2003**, *281*, 673–685.
(23) Witten, T. A.; Sander, L. M. *Phys. Rev. Lett.* **1981**, *47*, 1400–1403.
(24) Niu, Z.; Bruckman, M. A.; Li, S.; Lee, L. A.; Lee, B.; Pingali, S. W.; Thiyagaraja, P.; Wang, Q. *Langmuir* **2007**, *23*, 6719–6724. Rong, J.; Oberbeck, F.; Wang, X.; Li, X.; Oxsher, J.; Niu, Z.; Wang, Q. *J. Mater. Chem.* **2009**, *19*, 2841–2845.
(25) Pouget, E.; Dujardin, E.; Cavalier, A.; Moreac, A.; Valéry, C.; Marchi-Artzner, V.; Weiss, T.; Renault, A.; Paternostre, M.; Artzner, F. *Nat. Mater.* **2007**, *6*, 434–439.
(26) Tahir, M. N.; Natalio, F.; Berger, R.; Barz, M.; Theato, P.; Schröder, H.-C.; Müller, W. E. G.; Tremel, W. *Soft Matter* **2009**, *5*, 3657–3662.
(27) Deng, D.; Tang, R.; Liao, X.; Shi, B. *Langmuir* **2008**, *24*, 368–370.
(28) Sambrook, J.; Russell, D. W. *Molecular Cloning*, 3rd ed.; Cold Spring Harbor Laboratory Press: New York, 2001; Chap. 3.